

## **Chapter 6**

### **High Pressure Studies on some liquid crystals exhibiting Hexatic B/Crystal B Phases**

## 6.1 Introduction

High pressure is a very useful thermodynamical parameter in the study of liquid crystalline phase transitions and the associated critical phenomena, mainly because it permits us to probe single component systems[1]. One of the significant early results in the area of high pressure studies on liquid crystals was the observation of pressure induced mesomorphism[2] in materials which do not show liquid crystalline phases at atmospheric pressure. This led to the observation[2,3,4] of triple points (a triple point is the meeting point of three first order lines) at high pressure. The potentialities of investigating multicritical phenomena at high pressures were realised by the observation of a tricritical point (TCP) on smectic A - nematic (or cholesteric) boundaries[3,5]. Another important result was the observation of nematic-smectic A-smectic C (NAC) multicritical point at high pressures in a single component system[6] which was found to be topologically identical to the one obtained at room pressure in binary systems[7]. Yet another multicritical point that has been observed at high pressures is the reentrant nematic-smectic C-smectic A (RN-C-A) point[8]. Till recently no other types of multicritical points appear to have been observed in liquid crystalline systems at high pressures.

The work described in this chapter was undertaken with a view to observing possible new kinds of multicritical points at high pressures. In particular the systems chosen for study exhibited either hexatic B ( $B_{hex}$ ) or crystal B ( $B_{cry}$ ) phase, and as we shall see presently, the experiments have led to the observation of new phase diagrams involving critical end points.

We shall first describe the structures of the two modifications of the smectic B, referred to above, and also outline the essential features of critical end points (CEP) with some examples of such points observed in other condensed matter systems.

### 6.1.1 Smectic B

As discussed in Chapter 1, the smectic B liquid crystal is characterised by hexagonal order of the molecules within each layer. Two types of smectic B have been identified, viz., the crystal B phase and the hexatic B phase, the structures of which are described below.

Halperin and Nelson[9] proposed that a 2D solid should first melt into a phase characterised by long range bond orientational order, but short range positional order, and that this phase will then melt into a 2D isotropic fluid. The intermediate phase is referred to as the 'hexatic' phase. Subsequently Birgeneau and Litster[10] proposed that the transformation from crystal B (which it will be recalled has 3D long range translational order) to smectic A (which, as we have already seen, is a layered structure with no in-plane positional order or interlayer positional correlations) should take place via a hexatic B phase. This phase consists of stack of hexatic layers forming a structure with 3D long range bond orientational order, in-plane short range positional order and little or no interlayer positional correlations. High resolution X-ray studies by Pindak et al[11] on free standing films of *n*-hexyl -4'-*n*-pentyloxy biphenyl-4-carboxylate (65OBC) established existence of the hexatic B ( $B_{hex}$ ) supporting the model proposed by Birgeneau and Litster.

Bond orientational order is an essential property in defining hexatic phases and it is perhaps worthwhile explaining it in some detail. For a dense packing of spheres on a flat surface, which forms a perfect two dimensional triangular lattice of indefinite size, each sphere is surrounded by six neighbouring spheres, and each hexagon would be oriented in the same way throughout the lattice. This type of ordering, in which the hexagons are parallel everywhere, even when there is no lattice, is known as bond orientational order. The hexatic B phase is formed of a stack of such hexatic layers. In the case of molecular systems, the term 'bond' implies the line joining the centers of neighbouring molecules.

### 6.1.2 Critical End Point (CEP)

As we have already seen in Chapter III, the point at which a line of critical points (or a line of second order transitions) goes over to a line of first order transitions is a tricritical point (TCP). In terms of the Landau free energy expression,

$$F = F_0 + \frac{1}{2}aM^2 + bM^4 + cM^6$$

(where M is the order parameter) the TCP occurs when  $b = 0$  and  $c > 0$ . But this is not the only way a line of first order transitions and a line of second order transitions meet. Suppose in the above expression,  $b > 0$  and  $c < 0$ , then a 8th order term in M with a positive coefficient has to be added in order to stabilize the system. The resulting free energy,

$$F = F_0 + \frac{1}{2}aM^2 + bM^4 + cM^6 + dM^8$$

has been shown to give rise to a phase diagram of the kind given in Figure 6.1, where a line of second order transitions is truncated by meeting a line of first order transitions at a critical end point (CEP)[12]. Here  $H$  is the ordering field, for e.g., magnetic field for a metamagnet and  $T$  is the temperature. Experimentally only a few instances of critical end points have been reported, like for e.g., in [111]-stressed  $\text{RbCaF}_3$ [13], in  $\text{KMnF}_3$ [14],  $\text{CeSb}$ [15] etc. An example of a CEP has been reported in a temperature - concentration ( $T - X$ ) plane for a binary liquid crystalline system[16]. But a CEP had not been seen in a single component liquid crystalline system. Therefore the occurrence of such a point in single component systems is of considerable interest.

## 6.2 Experimental

### 6.2.1 Materials used

The structural formula and the transition temperatures of the materials used for the studies are given in Table 6.1. The material butyloxy benzylidene octyl aniline (4O.8) shows nematic- smectic A-crystal B phase sequence at room pressure. Heptyloxy benzylidene heptylaniline (7O.7) has smectic A-smectic C-crystal B phase transition and the 50 mol % mixture of 4- pentyloxy -4' -decyloxybenzoate (5OPDOB) and 4- heptyloxy -4' -decyloxybenzoate (7OPDOB) shows smectic A-smectic C-nematic B phase sequence at 1 bar.

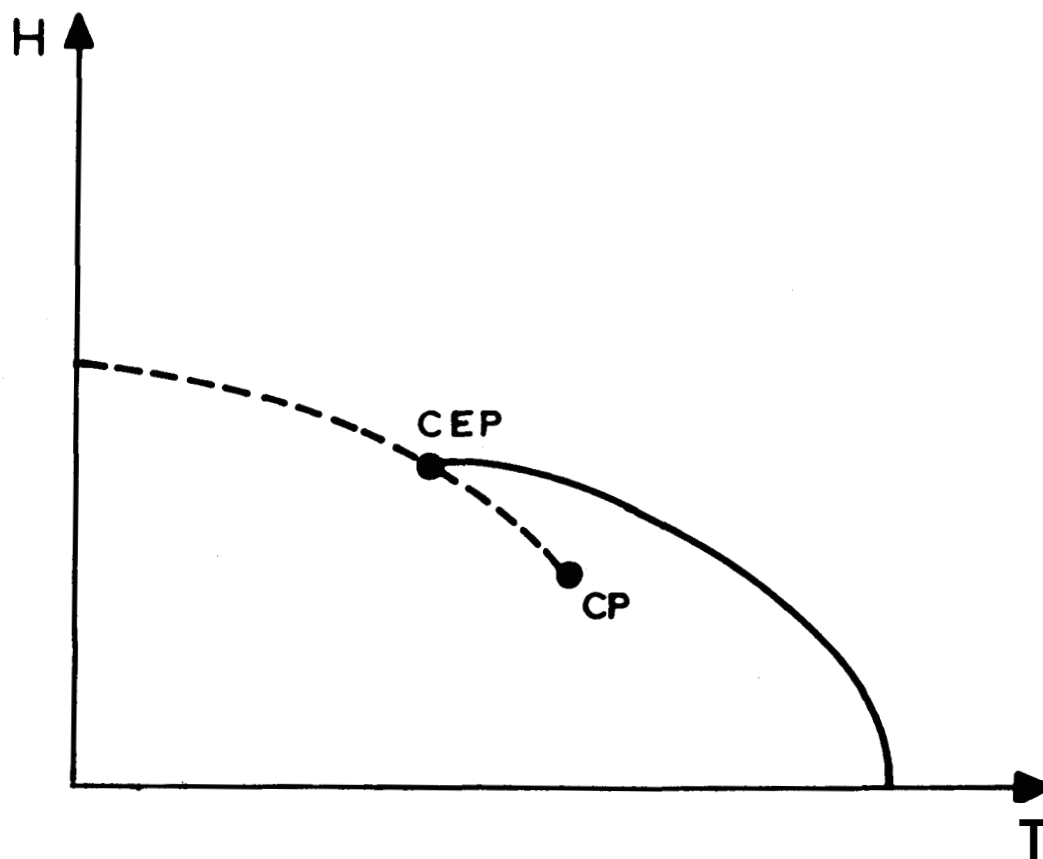
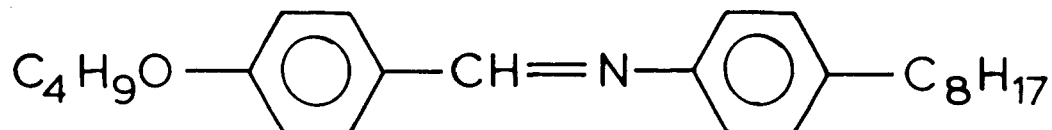


Figure 6.1: Phase diagram for the Critical End Point in the H-T plane.

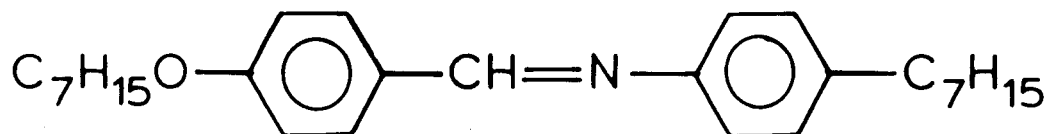
Chapter 6: High Pressure studies on some **liquid crystals**...

Table 6.1: Structural formulae and transition temperatures ( $^{\circ}\text{C}$ ) of the materials used.

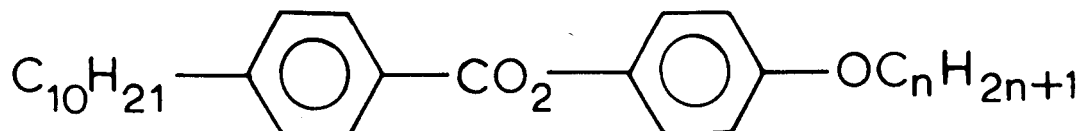
40.8



70.7



nOPDOB



Material	Iso	N	A	C	$B_{hex}$	$B_{cry}$
40.8	.	78.9	. 62.8	. -	-	. 48.2 .
70.7	.	83.8	. 83.5	. 71.5	. -	. 68.8 .
50% 5OPDOB and 7OPDOB	.	86.3	. 81.9	. 74.5	. 44.5	. -

Iso= isotropic phase, N = nematic,

A = smectic A, C = smectic C,

$B_{hex}$  = hexatic B,  $B_{cry}$  = crystal B.

## 6.2.2 High pressure set up

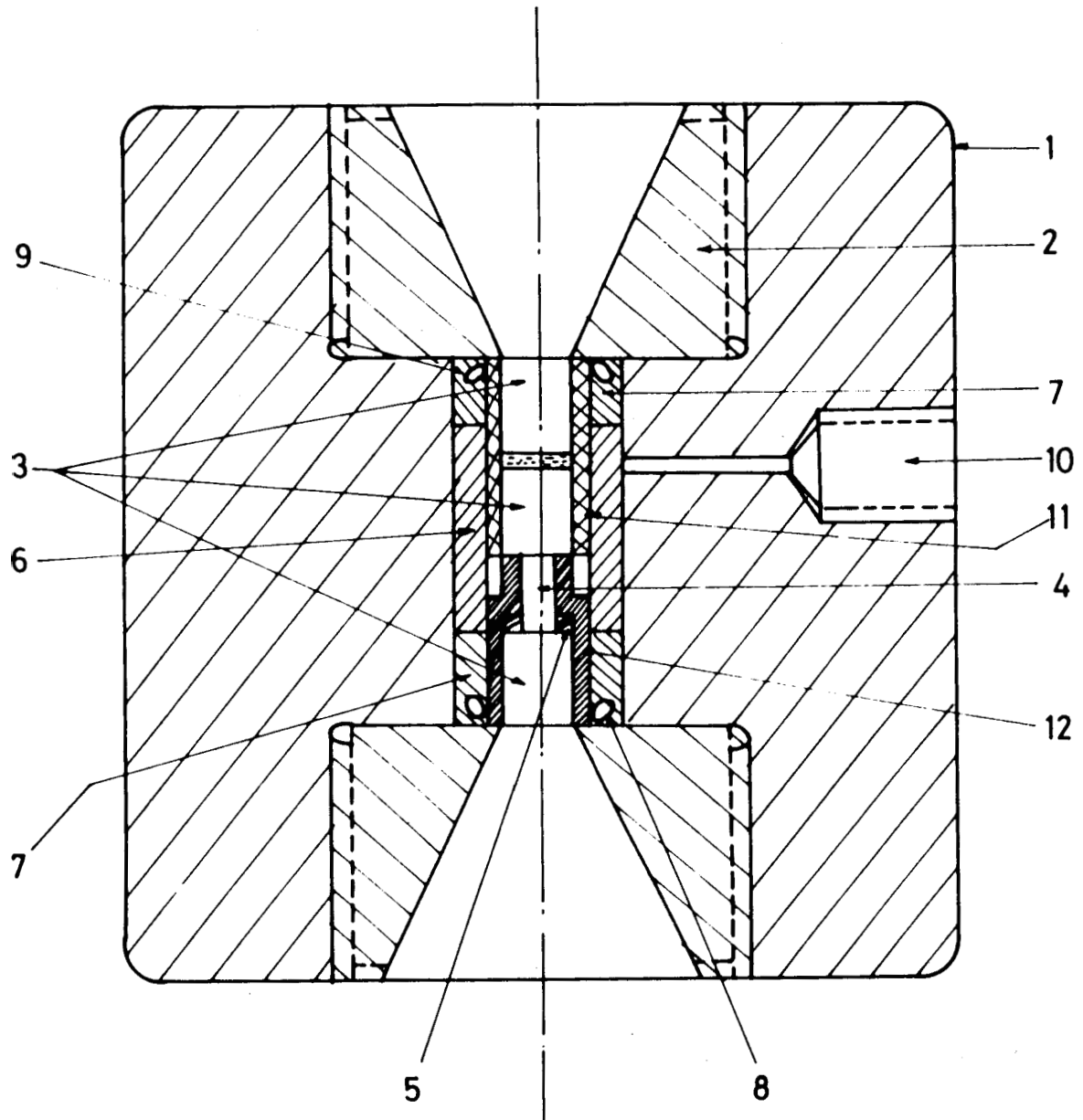
The experiments have been carried out using a calibrated high pressure optical cell, up to pressures of about 3 k bar. The pressure was generated using a pressure transmitting fluid (plexol). Since the set up already existed in our laboratory and has been described in great detail earlier [17], we shall only describe it briefly here. The only modification in the set up is that the data acquisition was done under computer control.

### High pressure optical cell

The schematic diagram of the cell is shown in Figure 6.2. The two important features of this cell are that

1. it can be used for both light scattering and optical microscopic experiments.
2. even small quantities of sample (<5 mg) can be used for the measurements.

All the components of the cell were machined out of a low alloy hardenable steel, viz., EN-24 which has 0.4 % carbon, 0.2% silicon and 0.55% nickel. The body of the cell (Figure 6.3) has threaded openings on both sides into which the two plugs (see Figure 6.3) with exactly matching threads can be fitted. On the outside the plugs have a large tapered opening (SO° outside taper) which facilitate the viewing without affecting the strength of the plug. On the inside, the plugs have small protrusion which are made optically flat by handlapping. These plugs keep the sample assembly in position. The hole in the cell body



1. CELL BODY      2. STEEL PLUG      3. SAPPHIRE CYLINDERS  
4. GLASS ROD      5. WASHER AND SPRING      6. CENTRE SPACER  
7. OUTER SPACER      8. 'O' RING      9. ANTIEXTRUSION RING  
10. HIGH PRESSURE CONNECTION      11. FLURAN TUBE      12. LOW-PRESSURE SEALER

Figure 6.2: High pressure optical cell.

Chapter 6: High Pressure studies on some liquid crystals...

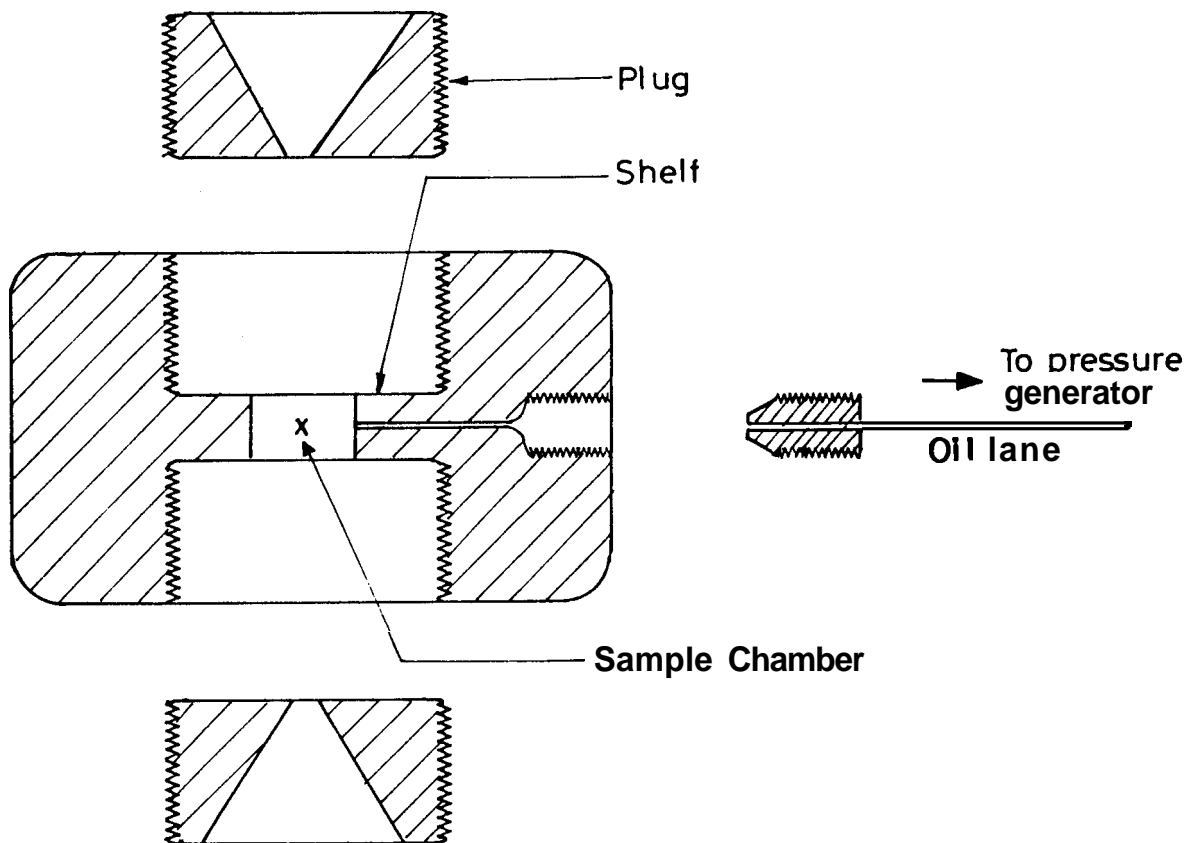


Figure 6.3: Schematic diagram of the basic parts of the high pressure cell.

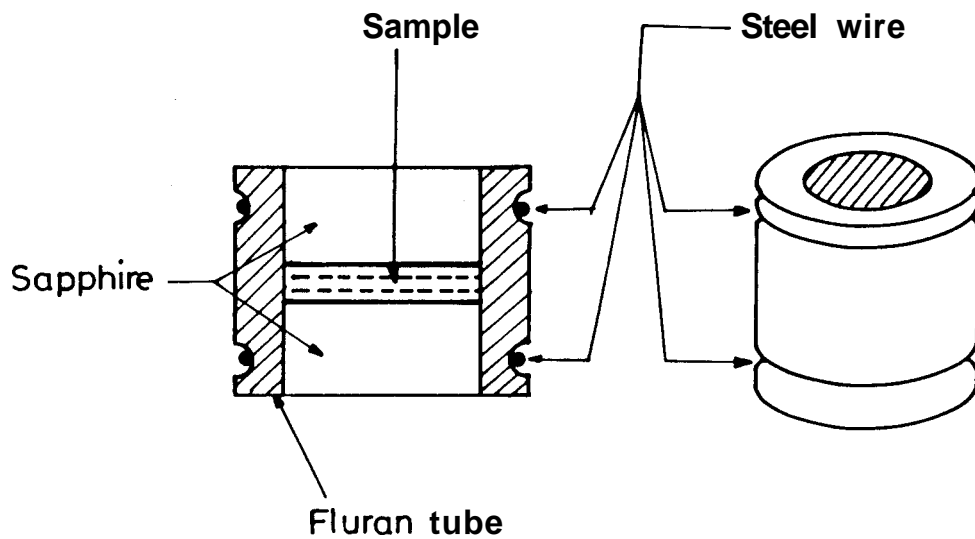


Figure 6.4: Sample assembly.

for the pressure connection consists of a smaller hole which extends from the interior of the body to about two - thirds of the thickness and joins a larger hole bored from outside.

In order to develop high pressure in the small central chamber it is essential to have a tight seal along both boundaries of the plugs. One for the central hole and the other along the circular boundary of the chamber against the plug. The seal at the central hole was made with optically polished sapphire windows and a small washer made of thin aluminium foil. The thin clearance between the plug and the sample chamber usually caused by a slight lifting of the plug at high pressure was avoided by placing around the junction a neoprene 'O' ring in conjunction with an antiextrusion ring.

### Sample encapsulation

The liquid crystals interact with the pressure transmitting fluid. Therefore, to isolate the sample from the pressure transmitting medium, a fluran tubing is used. Fluran, an elastomer, does not interact with liquid crystals and at the same time transmits pressure exceedingly well. It can also withstand temperatures upto 270 °C. The sample assembly is schematically represented in Figure 6.4. The sample was sandwiched between two sapphire rods which fit snugly inside the fluran tube. An effective seal was provided by tightly wrapping a thin steel wire around the tubing on the sapphire rods.

The inner spacer (low pressure sealer), washer and the spring (Figure 6.2) centre the bottom sapphire of the sample assembly and keep it under high ten-

sion. The third sapphire which was completely isolated from the sample assembly seals the bottom end of the pressure cell. The space between this third sapphire and the bottom sapphire of the sample assembly was occupied by a glass rod reducing thereby the amount of oil between these two sapphires which otherwise would have reduced the intensity of the transmitting light. All the three sapphire rods are specially cut such that the C-axis is perpendicular to the faces.

The heating system is made of an aluminium cylinder whose internal diameter is such that the pressure cell could be push-fitted into it. Nichrome tape is wound on mica sheets - which served as an electric insulator - the mica strips in turn were wrapped around the inside wall of the aluminium cylinder. A calibrated chromel-alumel thermocouple sheathed in a ceramic tube was used to measure the sample temperature.

### **6.2.3 High pressure plumbing system**

The schematic diagram of the high pressure plumbing system used in the present study is shown in Figure 6.5. A hand pump (PPI, USA) is used to generate the pressure in the cell. Fine variations of pressure are achieved by using a pressure generator (HIP, USA) with a small displacement capacity. The line pressure, which is nothing but the pressure experienced by the sample, is measured by a Bourdon type (HEISE) gauge. The plumbing connections are made through two-way and three-way valves. The valves as well as the tubing were chosen to withstand line pressures up to 7 kbar.

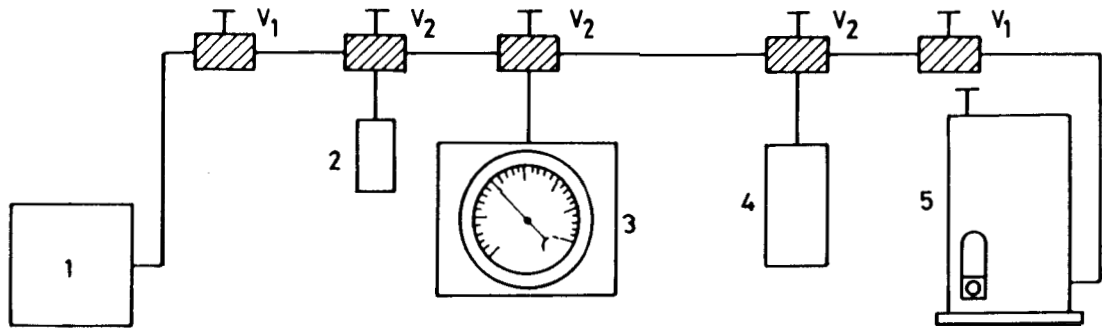


Figure 6.5: Schematic diagram of the high pressure plumbing system.

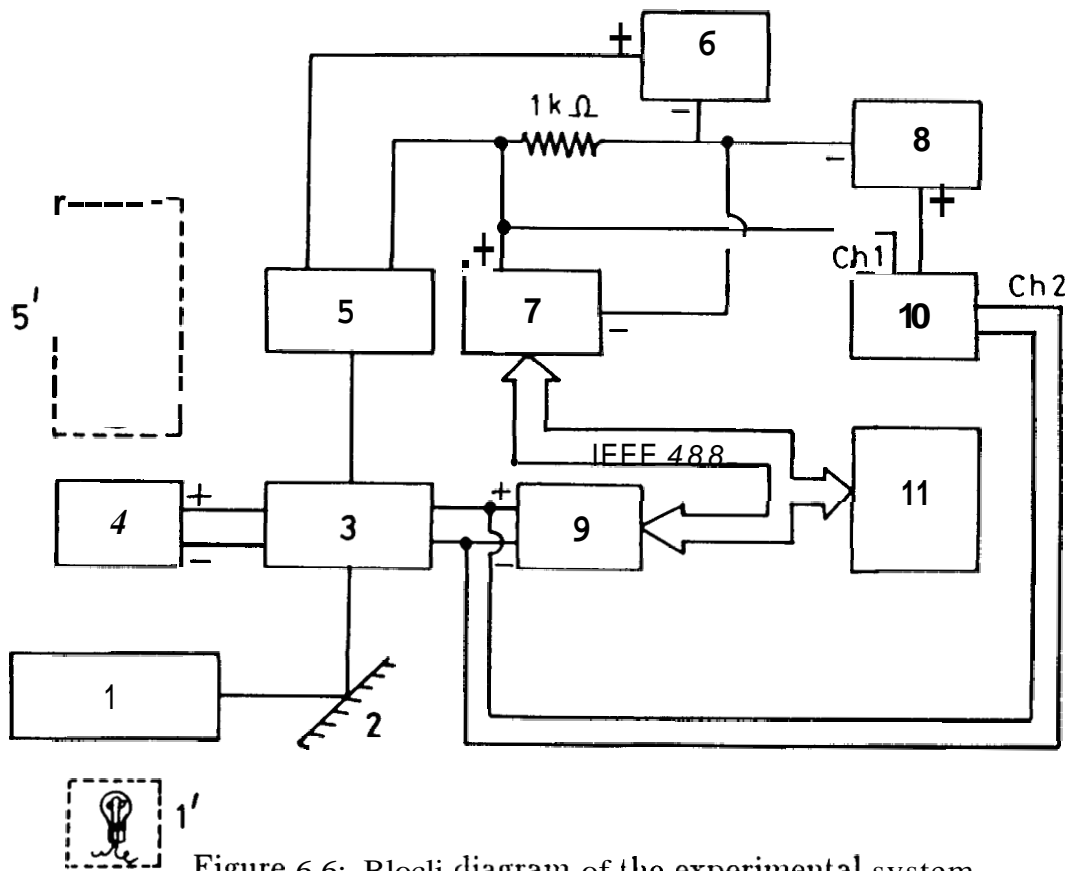


Figure 6.6: Block diagram of the experimental system.

1. He-Ne Laser, 2. mirror, 3. High pressure optical cell, 4. Heater power supply, 5. Photodiode, 6. Photodiode bias power supply, 7. Multimeter for measuring intensity, 8. D.C. Standard source used for voltage offset, 9. Multimeter for measuring the thermocouple output, 10. Multichannel recorder, 11. Microcomputer.

Instruments indicated by primed numbers are used for microscopic observations.

The sample was pressurised in a straightforward way. Pulling the handle of the hand pump raises the piston and draws oil from reserve into the pump's chamber. Pushing the handle down lowers the piston which compresses the oil and sends it through the steel oil line to the cell. After this 'priming' operation pressure could be fine controlled using the pressure generator. As the pressure in the cell is same as that in the pump, the cell pressure could be directly measured by measuring the line pressure. It was ascertained in earlier studies that the two are equal.

#### **6.2.4 A typical experiment**

The block diagram of the experimental set up is shown in Figure 6.6. Light from a He - Ne laser (Spectra Physics 5 mW) was made to fall on the sample in the optical cell. A photo detector was positioned to collect the light transmitted by the sample. The voltage drop across a fixed resistance ( $1\text{ k}\Omega$ ) caused by the current output of the detector was measured by a multimeter (Keithley model 174). A parallel connection from this, through a voltage source, was given to one of the channels of the multichannel recorder (Linseis model 2041) and also to a microcomputer. The temperature of the sample was measured by nanovoltmeter (Keithley 181). The output of this was given to another channel of the recorder as well as to the computer. Thus both the intensity and the temperature were monitored simultaneously and stored in the computer for the off-line analysis. Whenever a phase transition occurs there would be an abrupt change in the intensity of the transmitted light. The precision in measuring the pressure was  $\pm 0.8$  bar and the temperature  $\pm 20$  mK.

## 6.3 Results and Discussion

### 6.3.1 4O.8

The pressure-temperature (P-T) phase diagram for 4O.8 is shown in Figure 6.7. It is seen that as the pressure increases, the range of the A phase decreases, until finally it gets suppressed at about 2.8 kbar giving rise to a N - A - B<sub>cry</sub> meeting point. Beyond this pressure, the B<sub>cry</sub> phase transforms directly to the nematic phase.

High resolution X-ray and heat capacity studies[18] conducted on 4O.8 at 1 bar have shown that the A - N transition is second order. It has also been shown that A - B<sub>cry</sub> transition is first order[19] at atmospheric pressure. One of the earlier pressure studies[20] on this material have shown that the meeting point is a triple point. But high pressure studies by Stishov et al[21], (See Figure 6.8) showed a similar behaviour to ours. They have also carried out piezometric measurements[21,22] on volume change ( $\Delta V$ ) and also the entropy change ( $\Delta S$ ) associated with A - B<sub>cry</sub>, N - B<sub>cry</sub> as a function of pressure. The plot of volume and entropy change as a function of pressure for A - B<sub>cry</sub> and N - B<sub>cry</sub> transitions is shown in Figure 6.9. Their results showed that both A - B<sub>cry</sub> and N - B<sub>cry</sub> transitions are first order with large values of  $\Delta V$  and  $\Delta S$  right upto the meeting point. Also, the behaviour of thermal expansion across the A - N transition showed that this transition remains second order right upto the meeting point[22]. Thus the order of the transitions do not seem to be affected by the increasing pressure. These results indicate that the meeting point is a CEP.

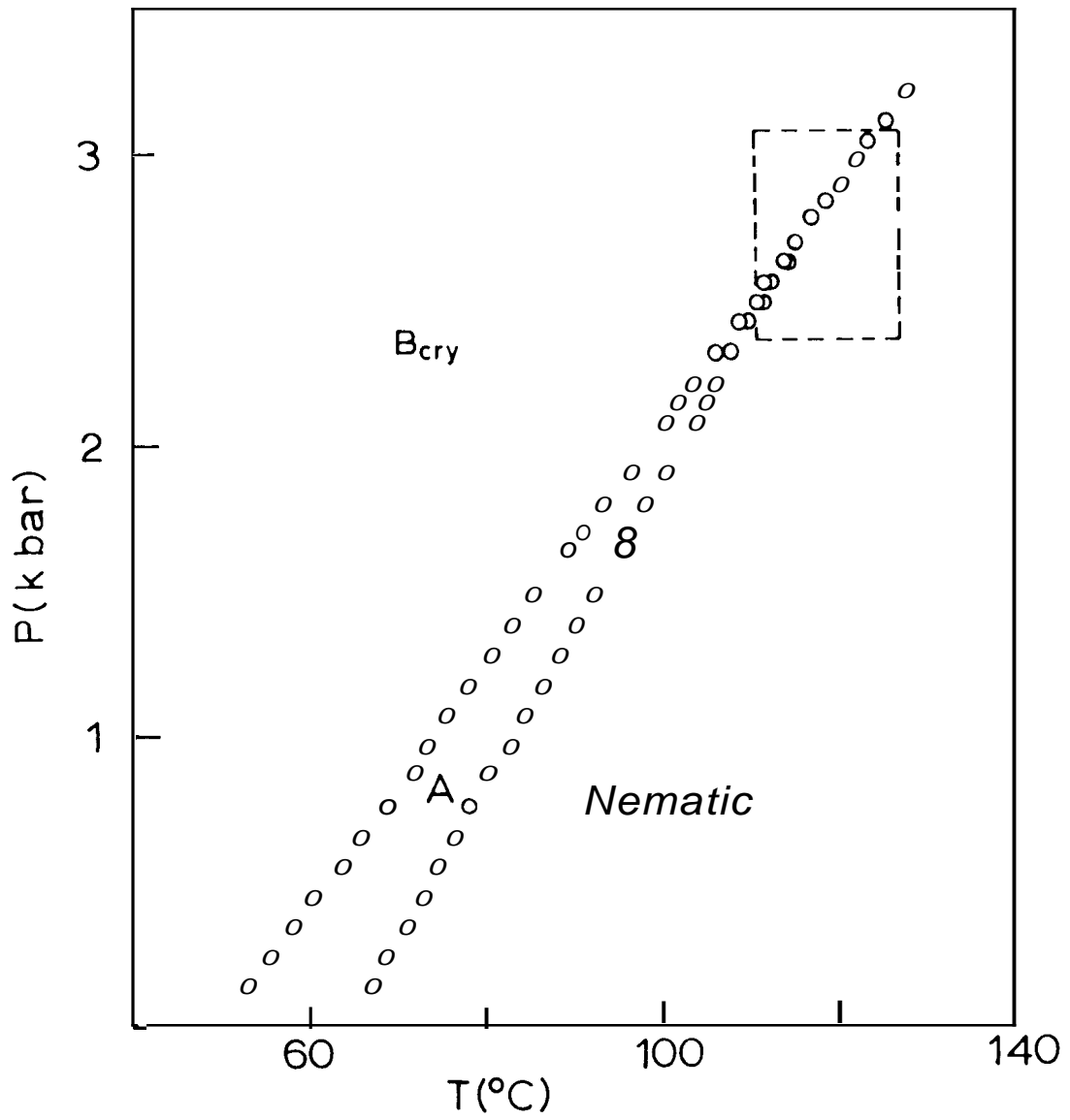


Figure 6.7: The pressure-temperature (P-T) phase diagram for 40.8.

Chapter 6: High Pressure studies on some liquid crystals...

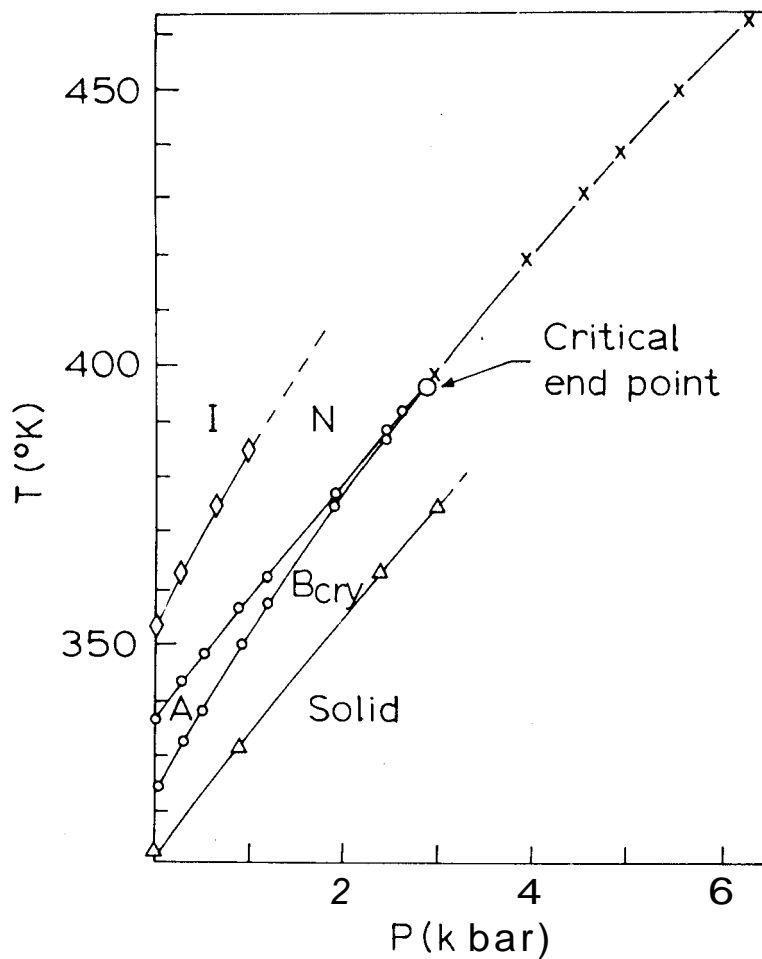


Figure 6.8: P-T diagram for 40.8 (from ref.[21]).

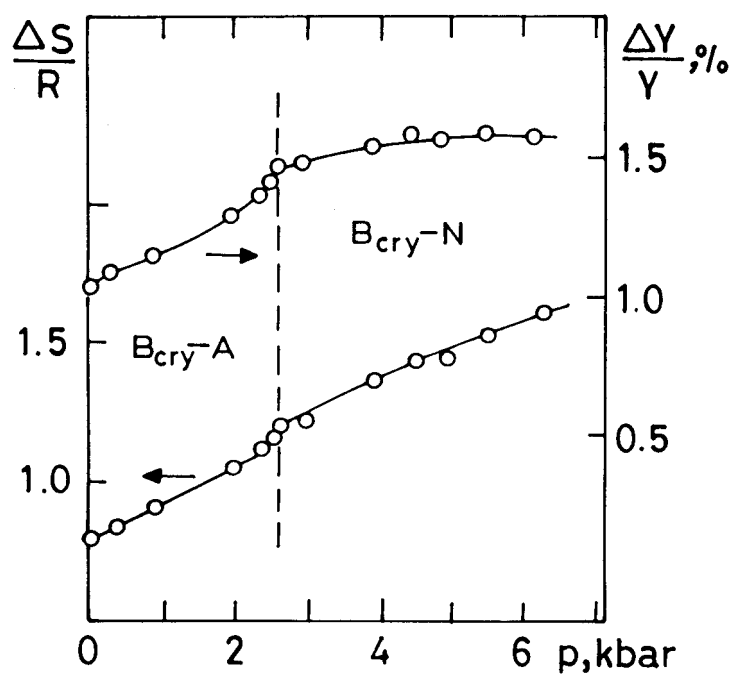


Figure 6.9: The plot of volume and entropy change as a function of pressure for A-B,, , and N-B<sub>crly</sub> transitions in 40.8.(from ref.[21]).

High resolution experiments have been carried out in the vicinity of the meeting point to see whether it is a CEP or not. The data is shown in Figure 6.10. It can be seen from the figure that the A -  $B_{cry}$  and the N -  $B_{cry}$  boundaries are collinear indicating that both have the same slope. The first order boundaries go through the CEP with out a change in slope[23]. Moreover, the topology of the phase diagram is very similar to what has been observed in the case of [111]-stressed  $RbCaF_3$ [13] (Figure 6.11) which shows a CEP in the P-T plane. These results confirm that the N - A -  $B_{cry}$  point is a Critical End Point.

As we know already, the  $B_{cry}$  phase has a 3D positional order, whereas, the A phase has 1D translational order and is fluid in the other two dimensions. On the other hand, the N phase has no positional order at all. Thus this CEP can be looked upon as a point at which there is a cross-over from a 2D melting to a 3D melting of positional order.

Despite considerable research efforts, N - A transition is not as well understood as the smectic A-smectic C (A - C) transition. The A - C transition, as discussed in previous chapters, is generally found to be second order mean-field-like in most of the materials[24]. With this in view, the following material viz., 70.7, having A - C -  $B_{cry}$  phase sequence at room pressure was chosen for high pressure studies.

### 6.3.2 70.7

The structural formula and the transition temperatures of 70.7 is given in Table 6.1. Calorimetric investigations[25] at atmospheric pressure have shown that

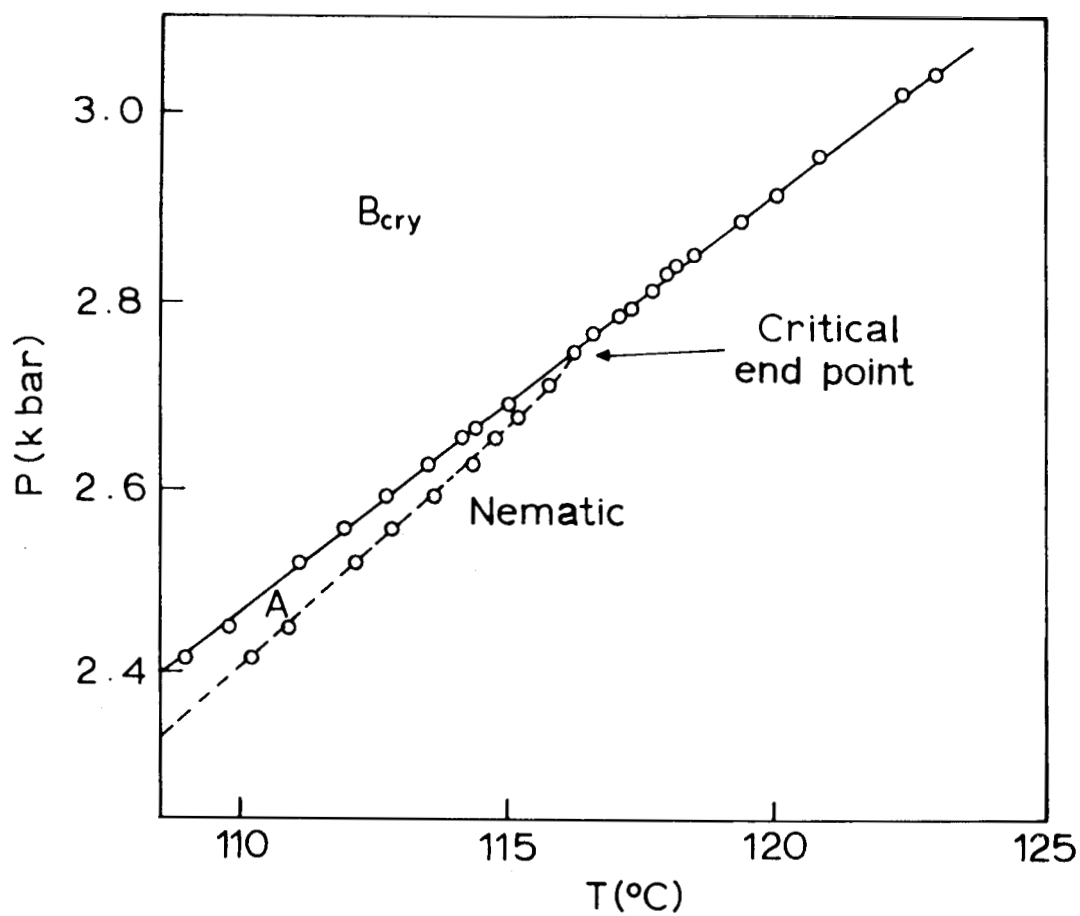


Figure 6.10: High resolution P-T diagram for 40.8.

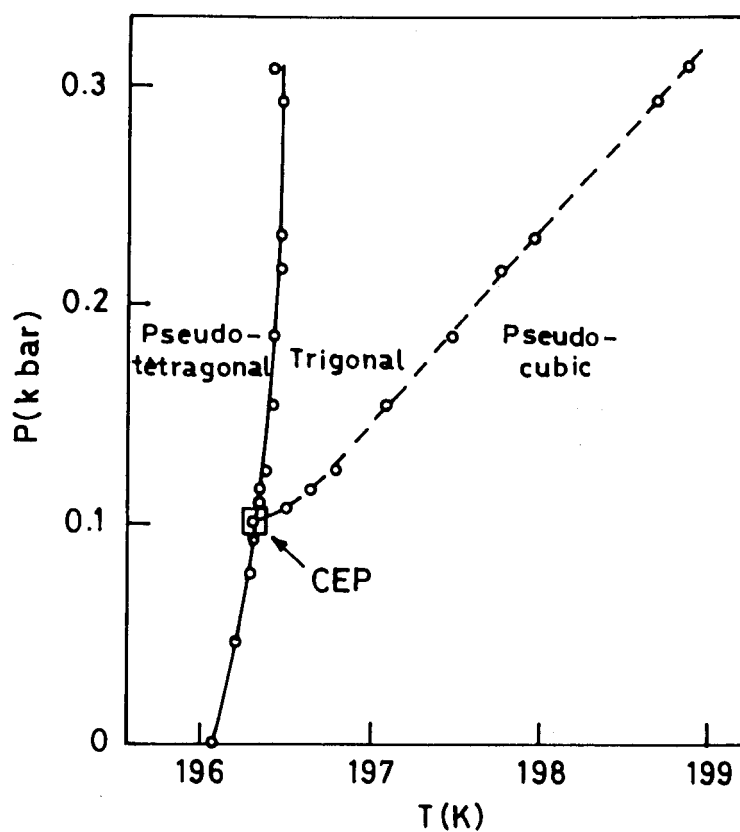


Figure 6.11: P-T diagram for [111]-stressed RbCaF<sub>3</sub>. (from ref.[13])

the A - C transition is second order and the C - B<sub>cry</sub> transition is first order for this compound.

The pressure-temperature (P-T) phase diagram for 70.7 is shown in Figure 6.12. As the pressure is increased the range of the C phase gets progressively smaller and it vanishes for pressures beyond 195 bar giving rise to a A - C - B<sub>cry</sub> point. To understand the nature of this meeting point, the phase diagram was mapped out in a greater detail near the meeting point. The topology of the phase diagram, shown in Figure 6.13, is very similar to that of 40.8 which showed a CEP. To quantitatively ascertain this the data was analysed in the following manner. The three boundaries A - C, C - B<sub>cry</sub> and A - B<sub>cry</sub> have been fitted to an equation of the form

$$|T_c - T| = A|P_c - P|^\eta + B|P_c - P| \quad (6.1)$$

(It may be mentioned here that this type of an expression has been used earlier[6] to describe the topology of the phase diagram near a NAC multicritical point.) Here T<sub>c</sub> and P<sub>c</sub> are the temperature and pressure corresponding to the meeting point, η is the exponent, A is the amplitude. The linear term on the right hand side serves to describe the background variation.

As pointed out in §6.3.1, for a CEP, the first order transitions go through the meeting point without a change in slope i.e., they should have the same value of η. From the Figure 6.13, it can be seen that the Equation 6.1 describes the data well for all the boundaries. Values of η, A and the coordinates of CEP, P<sub>c</sub> and T<sub>C</sub> are given in Table 6.2. Note that the exponent is the same for both C - B<sub>cry</sub> and A - B<sub>cry</sub> boundaries, while the A - C transition line has a different

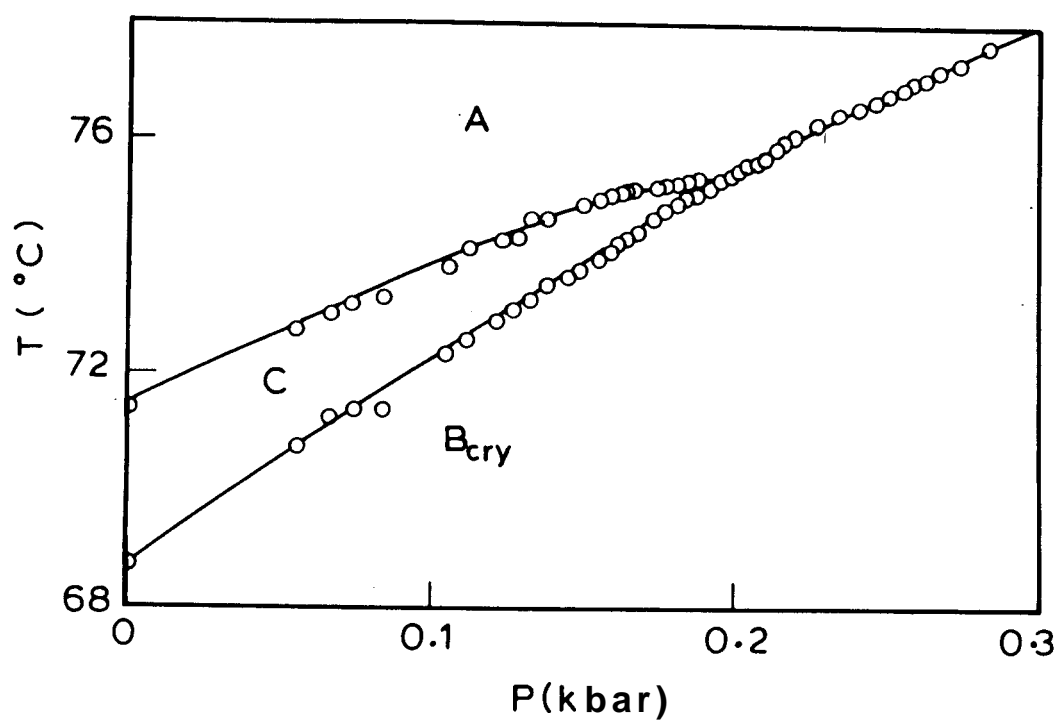


Figure 6.12: P-T diagram for 70.7. The solid lines are guide to the eye.

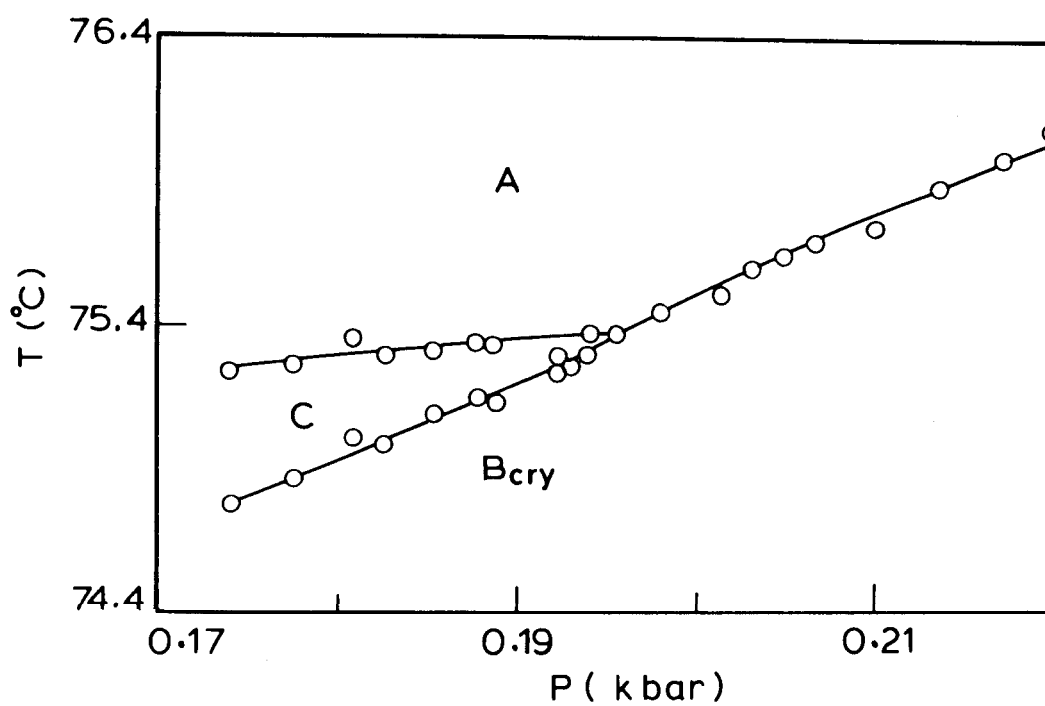


Figure G.13: High resolution P-T diagram for 70.7. The solid lines are fit to Equation 6.1.

Chapter 6: High Pressure studies on some *liquid crystals*...

Table G.2: Best fit parameters for individual fits of high resolution data for A - B<sub>crv</sub>, C - B<sub>crv</sub> and A - C phase boundaries for 7O.7

B	-0.0069
T <sub>c</sub>	75.38 ± 0.02 ° C
P <sub>c</sub>	195.726 ± 0.8 bars
$\eta_{A-B_{crv}} = \eta_{C-B_{crv}}$	0.93 ± 0.03
$\eta_{A-C}$	0.53 ± 0.03
$A_{A-B_{crv}}$	0.0426 ± 0.002
$A_{C-B_{crv}}$	-0.0253 ± 0.006
$A_{A-C}$	0.0072 ± 0.001

exponent. This shows that the C - B<sub>cry</sub> and A - B<sub>cry</sub> are collinear.

Room pressure measurements mentioned earlier indicate that C - B<sub>cry</sub> transition is first order and A - C transition is second order in this material. As for the A - C transition, only two parameters viz., transverse dipole moment of the constituent molecules and the temperature range of the A phase are known to change the order of the transition. The former may not be expected to change on application of pressure. At 1 bar itself the temperature range of the A phase is quite large and has been found to increase even further with increasing pressure. Thus the A - C transition can almost certainly be taken to remain second order right upto the meeting point. As far as the A - B<sub>cry</sub> transition is concerned, generally it has been found to be first order in all the materials studied so far. All the above evidence strongly indicate that the A - C - B<sub>cry</sub> point is a CEP.

It may be relevant here to recall the recent theoretical predictions of Fisher and Upton[26] regarding the topology of the phase diagrams near a CEP. The theoretical phase diagram is shown in Figure 6.14.  $g$  represents a nonordering field such as, for e.g., pressure, and  $T$  is the temperature. The crux of their argument is that the topology is universal and is related to the amplitude ratio  $\frac{A_+}{A_-}$  of the critical specific heat variation across the second order phase boundary. In particular, the curvature of the phase boundary should follow

$$\frac{d^2 P}{dT^2} \propto A_{\pm} |t|^{-\alpha}$$

where  $\alpha$  is the critical exponent for the specific heat variation. Thus the slopes of the first order lines C - B<sub>cry</sub> and A - B<sub>cry</sub> should mainly depend on the specific heat variation near the A - C transition. In a recent paper, Fisher and Barbosa

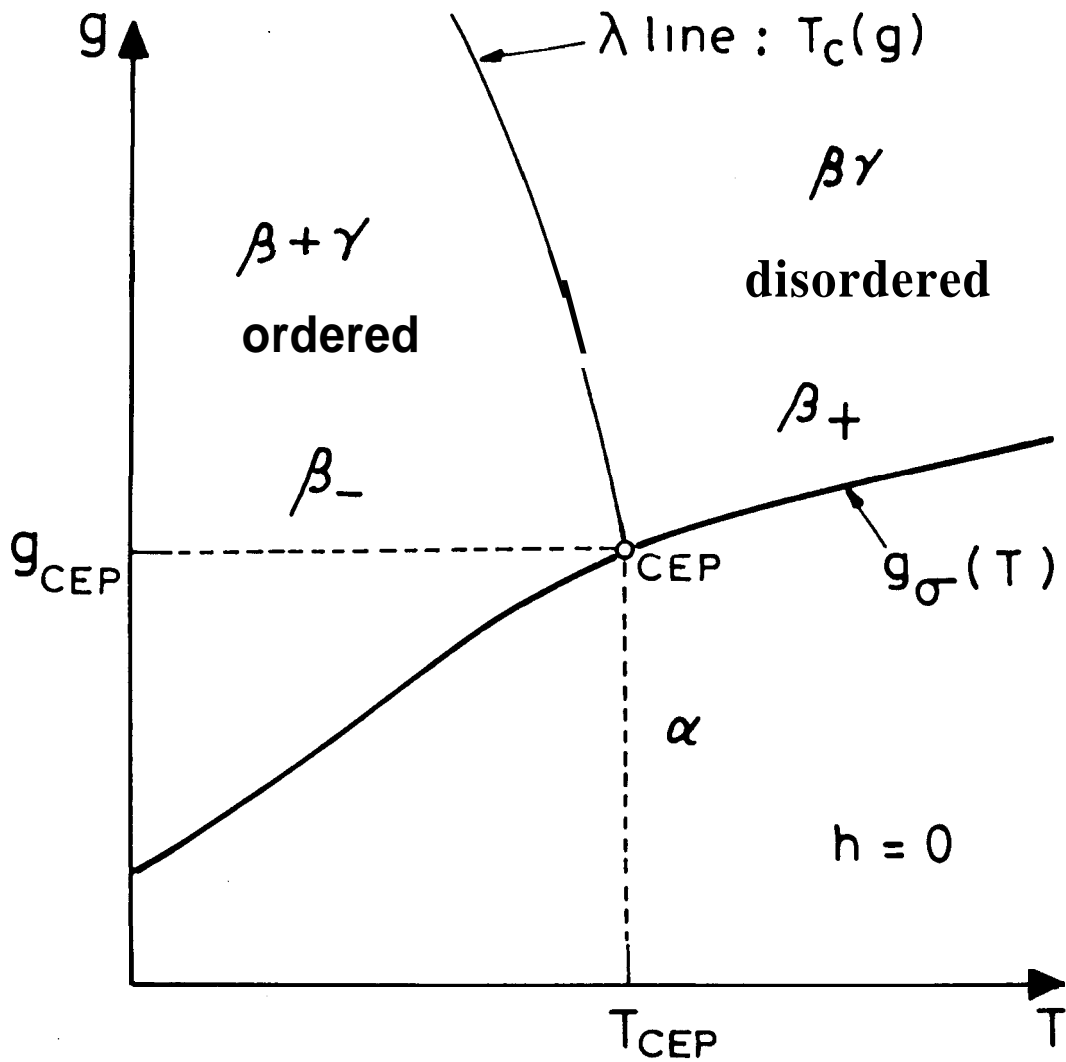


Figure G.14: Illustration of a critical end point at the join of a critical line  $\lambda$  and first order phase boundary,  $g=g_\sigma(T)$ , which separates the noncritical phase  $\alpha$  from ordered phase  $\beta_-$  and from the disordered phase  $\beta_+$  (from ref.[26]).

have commented[27] that for mean-field transitions even though  $A_+$  and  $A_-$  are not well defined, the specific heat exhibits a jump  $\Delta C_p$  at  $T_c$  and therefore the first order phase boundary,  $g_\sigma(T)$ , must display a jump in curvature at  $T_{CEP}$  which is proportional  $\Delta C_p$ . As mentioned earlier the A - C transition is almost always mean-field like and there is no reason to believe that this transition will become fluctuation dominated near the meeting point. The effect is to reduce the influence of the heat capacity on the curvature of the phase boundary. This explains the topology of the experimental P-T boundaries (Figure 6.13), which show, if any, only a very small deviation from linearity. Also from the fit values listed in Table 6.2 it can be noticed that the difference between the amplitude terms for A -  $B_{cry}$  and C -  $B_{cry}$  boundaries is small. Thus if at all there is any jump in the curvature for the first-order phase boundaries at the CEP, it would be too small to be noticed.

### 6.3.3 50 mol% of 5OPDOB and 7OPDOB

Having found a A - C -  $B_{cry}$  CEP under high pressure, the next step was to find a suitable material having a hexatic B( $B_{hex}$ ) phase instead of  $B_{cry}$  phase and a phase sequence A - C -  $B_{hex}$  at room pressure. The interest was to see whether the scenario seen in the case of 70.7 will be repeated or not. And if not, what would be the nature of the A - C -  $B_{hex}$  meeting point. Unlike the A- $B_{cry}$  and C -  $B_{cry}$  transitions, the A -  $B_{hex}$  and C -  $B_{hex}$  transitions, by symmetry arguments, can either be first order or second order. The material chosen for this study was 50 mol% of 5OPDOB and 7OPDOB, which showed the phase sequence A - C -  $B_{hex}$  at 1 bar. The reason for selecting the mixture instead of

the pure 4-hydroxy-4'-decyloxybenzoate (6OPDOB), which also exhibits the same sequence[28], was to stabilise the  $B_{hex}$  phase by lowering the crystallisation temperature. For all practical purposes the 50 mol% of 5th and 7th homologues of the nOPDOB series can be considered to be equivalent to the 6th homologue, because the basic chemical structure remains the same in both.

Room pressure calorimetric investigations[28,29] on the 5th, 6th and 7th homologues of nOPDOB series have shown that the A - C transition is second order in these materials. Also, the X-ray studies[28] on 6OPDOB have shown that the C -  $B_{hex}$  transition is first order. With these results in mind, it is safe to assume that the order of these transitions is the same for 50 mol% mixture at atmospheric pressure.

Figure 6.15 shows the P-T diagram for the 50 mol% mixture. Again the C phase gets suppressed as the pressure increases and vanishes at about 2.5 kbar. We have carried out high resolution studies near the A - C -  $B_{hex}$  point and the data are presented in Figure 6.16. The topology of the phase diagram looks very different from that of 7O.7. To know more about the nature of this point, data in the immediate vicinity of the meeting point was fitted to Equation 6.1. The  $\eta$  values obtained for the three boundaries are different. The values of  $\eta$  and amplitude A for the three boundaries and the pressure and temperature corresponding to the meeting point, are given in Table 6.3. The fact that the amplitude part of the non-linear term is extremely small compared to the linear term means that the A - C boundary, for all practical purposes, is linear near the meeting point. Both the A - C and A -  $B_{hex}$  boundaries are described well, also

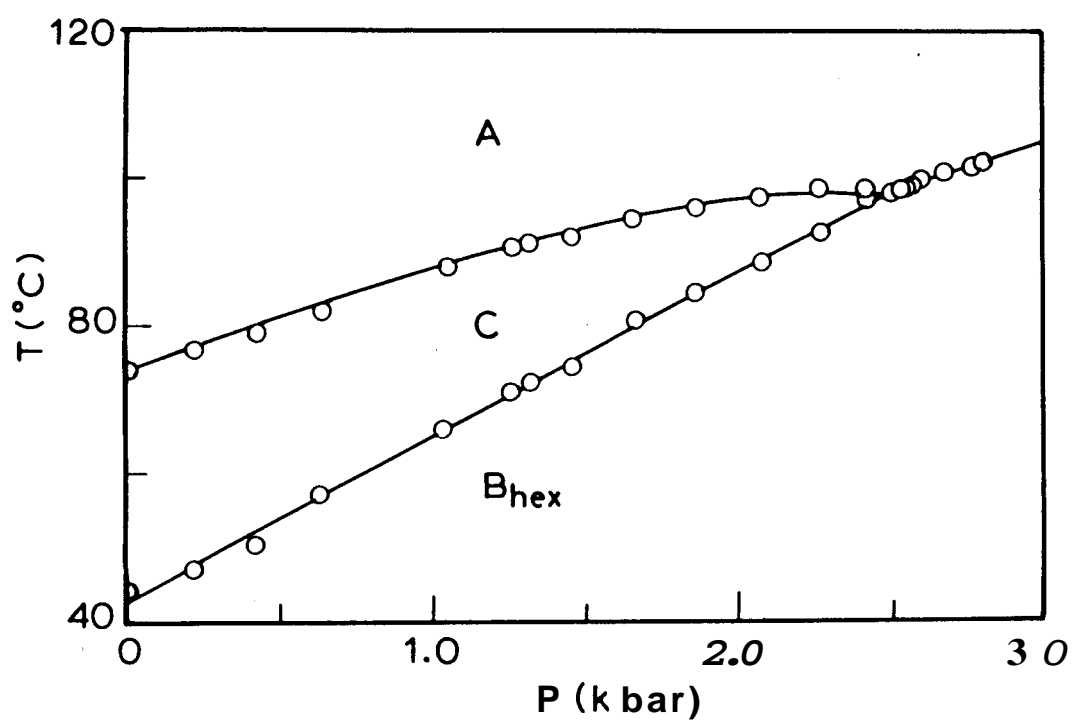


Figure 6.15: P-T diagram for 50 mol% 5OPDOB/7OPDOB. The solid lines are guide to the eye.

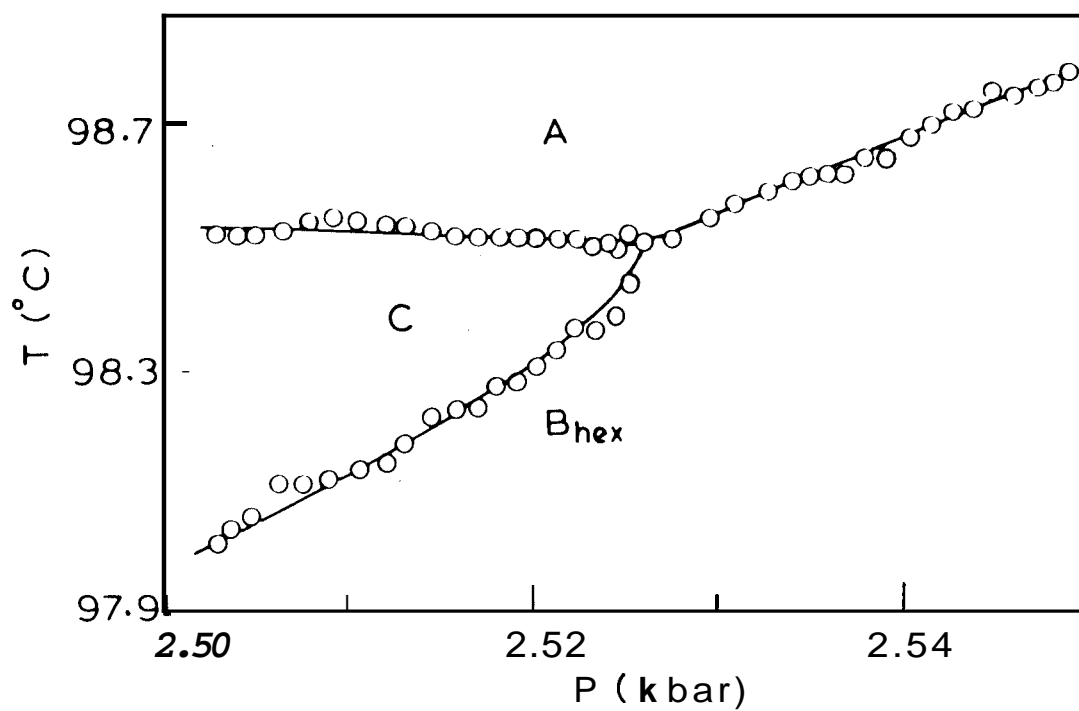


Figure 6.16: High resolution P-T diagram for 50 mol% 5OPDOB/70PDOB. The solid lines are fit to Equation 6.1.

Chapter 6: High Pressure studies on some liquid crystals...

Table 6.3: Best fit parameters for individual fits of high resolution data for A -  $B_{hex}$ , C -  $B_{hex}$  and A - C phase boundaries for 50 mol% of 5OPDOB and 7OPDOB

B	0.0014
$T_c$	$98.52 \pm 0.02$ ° C
$P_c$	$2526.14 \pm 0.8$ bars
$\eta_{A-B_{hex}}$	$0.99 \pm 0.03$
$\eta_{C-B_{hex}}$	$0.72 \pm 0.03$
$\eta_{A-C}$	$0.63 \pm 0.03$
$A_{A-B_{hex}}$	$0.0113 \pm 0.003$
$A_{C-B_{hex}}$	$-0.0548 \pm 0.005$
$A_{A-C}$	$0.0001 \pm 0.00005$

by straight line fits. Since the exponents are different for A -  $B_{hex}$  and C -  $B_{hex}$  boundaries, the possibility of a CEP can be ruled out.

Before discussing the other possibilities for the A - C -  $B_{hex}$  meeting point it is relevant to mention here about the theoretical predictions of Bruinsma and Nelson[30]. They have predicted a multicritical point in the mean-field phase diagram of a coupled system of bond- and tilt- orientation angles. The phases involved are the same as in our system, i.e., A, C and stacked hexatic B phases. The phase diagram in the plane of inverse dimensionless stiffness constants  $K_6^{-1}$  and  $K_1^{-1}$  is shown schematically in Figure 6.17.  $K_6$  measures the coupling between neighboring bond orientations, while  $K_1$  characterises the interaction between the nearby tilt angles. In their phase diagram all the three phases meet at a multicritical point, marking the termination of three XY - like lines of second order transitions. Notice that when the C phase has developed a large hexatic order, i.e., small  $K_6^{-1}$  value (left bottom of the figure), the phase could be similar to tilted hexatic phases smectic I or smectic F. It is not clear from Bruinsma and Nelson's paper whether there is a continuous evolution between the C phase to this tilted state with a large amplitude for the bond orientational order.

As mentioned earlier, in most of the materials it has been found that the A - C transition is second order and mean-field-like. But the nature of the A -  $B_{hex}$  and C -  $B_{hex}$  is not very clear. Heat capacity measurements have shown that A -  $B_{hex}$  transition in a number of materials is continuous with a large critical exponent associated with the specific heat anomaly[24]. As already mentioned the room pressure investigations indicated that A - C and the C -  $B_{hex}$  transitions

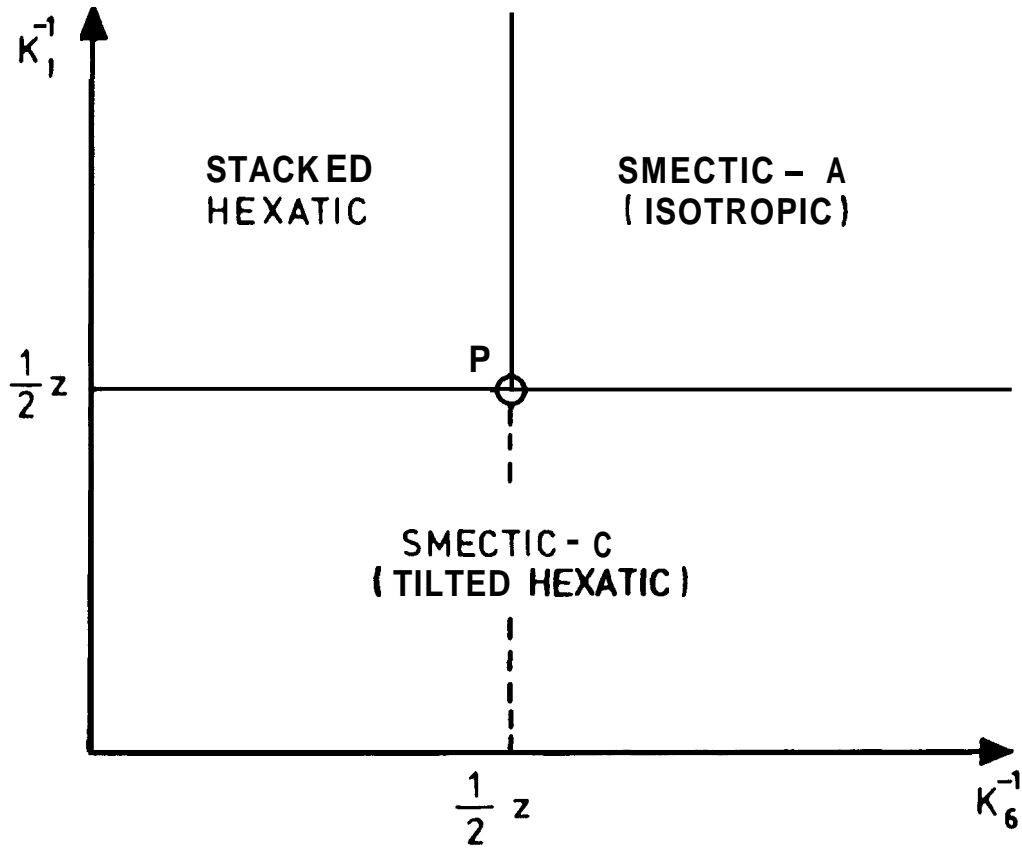


Figure G.17: Schematic phase diagram of a coupled system of bond- and tilt-orientation angles in the mean-field approximation. Different phases are shown as a function of inverse dimensionless stiffness constants  $K_6^{-1}$  and  $K_1^{-1}$  (from ref.[30]).

in this mixture is second and first order respectively. Using the same arguments as in the case of 70.7, the A - C transition near the A - C -  $B_{hex}$  point can be considered to be second order. Now, the following are the different possibilities for the meeting point.

1. If the order of the transitions do not change near the meeting point then it could be a mean-field bicritical point (The meeting point of two second order lines and one first order boundary).
2. If the C -  $B_{hex}$  transition becomes second order then the meeting point will be a new type of multicritical point.
3. If both A - C and A -  $B_{hex}$  transitions become first order then it would be a triple point. It may be noted here that, recently it was observed, 'that in the proximity of a smectic A-smectic C-smectic F meeting point, the A - C transition changed over from second to first order[31].

Thus the results of high pressure studies on materials exhibiting hexatic B/crystal B phases have led to the observation of a N - A -  $B_{cry}$  CEP, a A - C -  $B_{cry}$  CEP and a A - C -  $B_{hex}$  meeting point which has yet to be characterised unambiguously.

## References

- [1] For a review of high pressure studies of liquid crystals till 1978, see S. Chandrasekhar and R. Shashidhar, *Advances in liquid crystals*, 4, 83 (1979).
- [2] S. Chandrasekhar, S. Ramasheshan, A. S. Reshamwala, B. K. Sadashiva, R. Shashidhar and V. Surendranath, *Proc. Int. Liq. Cryst. Conf. Bangalore 1973; Pramana Suppl.*, 1, 117 (1975).
- [3] R. Shashidhar and S. Chandrasekhar, *J. Phys. (Paris)* **36**, C1-49 (1975).
- [4] R. Shashidhar, *Mol. Cryst. Liq. Cryst.* 43, 71 (1977).
- [5] P. H. Keyes, H. T. Weston and W. B. Daniels, *Phys. Rev. Lett.* **31**, 628 (1973).
- [6] R. Shashidhar, B. R. Ratna and S. Krishna Prasad, *Phys. Rev. Lett.* 53, 2141 (1984).
- [7] D. Brisbin, D. L. Johnson, H. Fellner and M. E. Nubert, *Phys. Rev. Lett.* 50, 178 (1983).
- [8] R. Shashidhar, A. N. Kalkura and S. Chandrasekhar, *Mol. Cryst. Liq. Cryst. Lett.* **82**, 311 (1982); R. Shashidhar, S. Krishna Prasad and S. Chandrasekhar, *Mol. Cryst. Liq. Cryst.* 103, 137 (1983).
- [9] B. I. Halperin and D. R. Nelson, *Phys. Rev. Lett.* 41, 121 (1978).
- [10] R. J. Birgencau and J. D. Litster, *J. Phys. Lett. (Paris)* **39**, 399 (1978).

- [11] R. Pindak, D. E. Moncton, S. C. Davey and J. W. Goodby, *Phys. Rev. Lett.* **46**, 1135 (1981).
- [12] T. A. L. Ziman, D. J. Amit, G. Grinstein and C. Jayaprakash, *Phys. Rev. B* **25**, 319 (1982).
- [13] J. E. Buzare, W. Berlinger and K. A. Muller, *J. Physique Lett.* **46**, 201 (1985).
- [14] K. Fossheim, *Multicritical Phenomena*, ed. R. Pynn and A. Skjeltrop, NATO Advanced Studies Institute, Series B: Physics Vol **106** (Plenum, N. Y., 1984); J. E. Buzare, W. Berlinger and K. A. Muller, *J. Phys. (Paris) Lett.*, **46**, L201 (1985).
- [15] B. Halg, A. Furrer and O. Vogt, *Phys. Rev. Lett.* **57**, 2745 (1986).
- [16] V. N. Raja, R. Shashidhar, B. R. Ratna, G. Heppke and Ch. Bahr, *Phys. Rev. A* **37**, 303 (1988).
- [17] S. Krishna Prasad *High Pressure Studies of Liquid Crystalline transitions*, Ph. D. Thesis, University of Mysore, 1985.
- [18] R. J. Birgeneau, C. W. Garland, G. B. Kasting and B. M. Ocko, *Phys. Rev. A* **24**, 2624 (1981).
- [19] P. S. Pershan, G. Aeppli, J. D. Litster and R. J. Birgeneau, *Mol. Cryst. Liq. Cryst.* **67**, 205 (1981); C. C. Huang, J. M. Viner, R. Pindak and J. W. Goodby, *Phys. Rev. Lett.* **46**, 1289 (1981).

- [20] P. E. Cladis and J. W. Goodby, *Mol. Cryst. Liq. Cryst. Lett.* 72, 307 (1982)
- [21] S. M. Stishov, S. N. Nefedov and A. N. Zisman, *JETP Lett.* 36, 348 (1982).
- [22] S. N. Nefedov, A. N. Zisman and S. M. Stishov, *Sov. Phys. JETP* 59, 71 (1984).
- [23] J. C. Wheeler, *J. Chem. Phys* 61, 4474 (1974)
- [24] C. C. Huang, *Theory and Applications of liquid crystals*, p. 185, Edited by J. L. Ericksen and D. Kinderlehrer, Springer-Verlag, N.Y., (1987).
- [25] J. Thoen and G. Seynhaeve, *Mol. Cryst. Liq. Cryst.* 127, 229 ( 1985).
- [26] M. Fisher and P. J. Upton, *Phys. Rev. Lett.* 65, 2402 (1990).
- [27] M. Fisher and M. C. Barbosa, *Phys. Rev. B* 43, 11177 (1991).
- [28] P. Keller, P. E. Cladis, P. L. Finn and H. R. Brand, *J. Physique* 46, 2203 (1985).
- [29] A. N. Kalkura *High Pressure Optical Studies of Liquid Crystals*, Ph. D. Thesis, University of Mysore, 1982.
- [30] R. Bruinsma and D. R. Nelson, *Phys. Rev. B* 23, 402 (1980).
- [31] V. N. Raja, D. S Shankar Rao and S. Krishna Prasad, *Phys. Rev. A*, 46, 726 (1992).